Design and realization of a Sphere Soft Valve

Carlo Bosio

Abstract

In this report are shown and explained the fundamental concepts that led to the idea for a soft material security valve. The aim of the element is to prevent the depressurization of a hydraulic system as a result of a damage to a circuit section. The analysis starts with feasibility evaluation with approximated structural and hydraulic models and then is deepened with valve mechanical design and FEM load and fluidic simulations. The fabrication procedure is also described, explaining the design of the mold for silicone injection.

1 Introduction

A frequently used actuation solution in soft robotics are pneumatic actuators. Despite their advantages, a common problem is their rupture. In fact, caused by the handmade fabrication and intrinsically by the use of soft materials, the risk of damaging is very considerable. In the particular scenario of this study, as soft actuating solution, McKibben muscles has been used, but possible applications of the developed valve could be many.

1.1 McKibben muscles

McKibben artificial muscles are a subclass of soft pneumatic actuators. They are composed by an internal inflatable chamber (usually made of silicone or other soft polymers) surrounded by two cylindrical helicoidal meshes of fibers that envelope the soft chamber in opposite directions (leftwards and rightwards). Depending of the helix angle of the two fiber meshes, several actuator behaviors can be obtained. This characteristic makes them very peculiar and very adaptable for different types of soft robotics actuation.

1.2 System description

The system for which the valve has been conceived consisted of a closed hydraulic circuit working between two pressure values (both greater than atmospheric pressure) for biomedical applications. As represented in Fig.1, McKibben muscles are powered by a single pressure source, and are thus comparable to parallel branches in the circuit. Consequently, without a preventing system, if one soft actuator breaks the whole system depressurizes, causing all other actuators' failure. In order to take up the minimal amount of space and guarantee good system reliability it was necessary to implement an entirely mechanical security system. Therefore, the purpose of this study was to conceive and analyse an effective solution for the exposed problem in order to avoid hydraulic circuit failure in case of catastrophic rupture of a soft actuator.

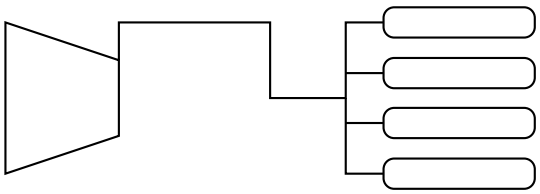

Figure 1: General system scheme

Among existing literature, almost nothing has been conceived and developed in terms of practical solutions observing the given constraints. Napp et al. in [1] study a passive valve based on a soft material flap, allowing flow in the forward direction but only a certain amount of backward flow before closing. Gilbertson et al. in [2] achieve similar results with an asymmetrical cracking pressure soft structure that acts like a two-way check valve. Soft passive valves have been used also by Shepherd et al. in [3], molded into the body of soft robots to study rapid actuation with internal explosions. In all the previous studies the valves are able to take advantage of a pressure gradient but didn't achieve hold states. Softe valves are widely used and developed also in microfluidic devices, as shown by Jiang and colleagues in [4], but principally with the aim of flow control by pneumatic or electrical signals. The objective of this study is to develop a bistable valve able to allow flow in both directions and obstruct a tube (permanently) if an excessive pressure gradient arise (soft actuator rupture).

2 Methods and models

The pumping system works between a maximum pressure of 2 bar (necessary for the pressure source to inflate the actuators) and a minimum pressure of $1,1$ bar. The outside of the system is essentially at atmospheric pressure (1 bar).

2.1 Concept

The main idea was to insert in every McKibben muscle inflating tube a soft material bistable valve, that could take advantage of a pressure gradient to obstruct the flow. In this way it would be possible, sacrificing one branch, to guarantee the hydraulic circuit functioning. Therefore, the situation that had to be analysed (illustrated in Fig.2) was the circumstance in which downstream of the valve there is atmospheric pressure and upstream there is the maximum pumping pressure, which is indeed the case of maximum risk of rupture.

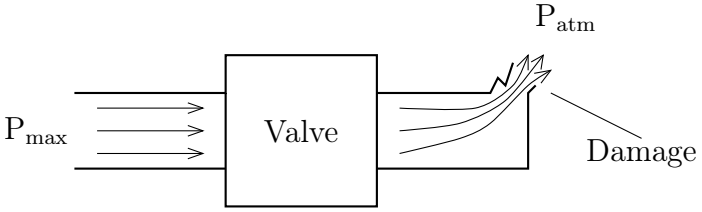

Figure 2: Catastrophic rupture in most stressful situation

2.2 First approach

The basic idea was to develop a system with a spherical element, because of its simple geometry and ease of production. The system has to let the flow circulate in working conditions and take

advantage of the overpressure between the two sides to obstruct the branch and isolate the damaged actuator. The most intuitive way to do that is to insert an element made of an elastomeric material able to stop the spherical element when pushed by the action of working pressure and compliant enough to let it through when exposed to the overpressure. A first attempt to put into practice this principle is represented in Fig.3.

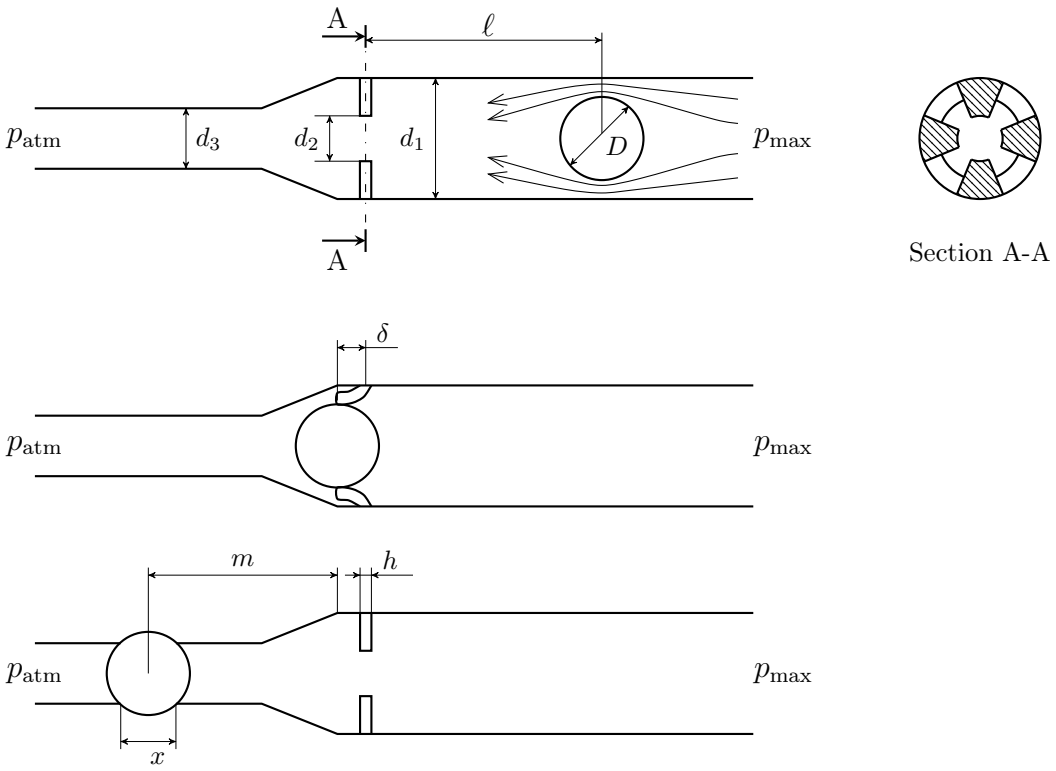

Figure 3: First approach operating principle

As represented in Fig.3, the sphere is inserted in a two-diameter cylindrical element. In normal operating conditions, the sphere oscillates in the right part (larger diameter). In particular, when the pressure source inflates the actuators, the sphere is pushed towards the left part, but it is stopped by the elastic fins. When the actuators are deflated, the sphere is dragged back to the right part by the flow. In these conditions the flow is free to pass through the free space between the sphere and the tube. The elastic fins have to be stiff enough to keep the sphere in the right part with normal operating pressures. When the rupture occurs the pressure gradient (1 bar) pushes the sphere, that pass through the elastic fins and get stuck in the smaller diameter part. Materials and dimensions of the system have to be calculated to guarantee this operating principle and obviously a blocking element should be provided to forbid the sphere to go away in the right part.
The cylindrical element is a thermoplastic tube with $d_1 = 5\,\text{mm}$ and thickness t. Referring to Fig.3, ℓ is the initial sphere stroke, m is the sphere penetration distance in the smaller diameter part. As a first approximation, it is possible to consider the fins having a linear elastic beam behavior which, assuming a generic force F can be modeled as follows, referring to Fig.4:

$$F = ky \tag{1}$$

Where k is the elastic constant of the equivalent spring. Using the formulas for a straight cantilever beam loaded with a bending force at the end (Galileo's Problem):

$$y = \frac{Fl^3}{3EJ_x} \tag{2}$$

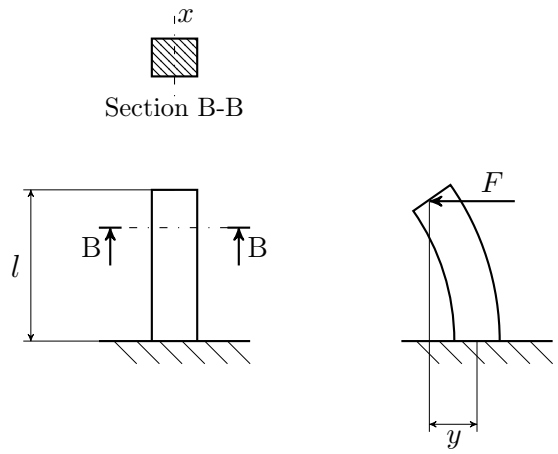

Figure 4: Linear elastic beam model

Where J_x is the section moment of inertia with respect to x axis and E is the Young modulus of beam material. From the two previous formulas result that:

$$k = \frac{3EJ_x}{l^3} \tag{3}$$

It is possible to extend this model to the elastic fins, taking into account that the results will be affected by very consistent errors. In fact small displacements and linear elasticity hypothesis (essential for the formulas above) are not verified in the case of the fins. This approximation provides just the order of magnitude of the involved quantities and allow to figure out the feasibility of this solution. With regard to the elastic fins it turns out to be:

$$\begin{aligned} l &= \frac{d_1 - d_2}{2} \\ J_x &= \frac{1}{12} b h^3 \end{aligned} \tag{4}$$

With b is indicated the mean circumferential width of a fin. Assuming the fins to cover half of the perimeter of a generic circumference concentric with the tube and calculating the total stiffness of an equivalent elastic element, the term b of each fin adds up to the others giving as result the length of the half-circumference with radius $\frac{1}{2}(d_1 + d_2)$.

$$k = \frac{\pi E h^3 (d_1 + d_2)}{2(d_1 - d_2)^3} \tag{5}$$

And by simple geometrical calculus:

$$\delta = \frac{1}{2}\sqrt{D^2 - d_2^2} \tag{6}$$

With the aim of writing a simple equation that, in a first approximation, could describe the system functioning principle, it is possible to write the energy balance equation. As showed in Fig.3, the sphere has an initial stroke of ℓ during which the pressure gradient pushes it towards the left side. The sphere bends the elastic fins (displacement δ) and pass through, getting stuck into the left part of the tube (after covering a short distance m) because of friction. The equation is:

$$\frac{\pi D^2}{4}(p_{\max} - p_{\text{atm}})(\ell + \delta + m) = \frac{1}{2}k\delta^2 + W_f \tag{7}$$

Where W_f is the energy dissipated by friction action between the smaller tube part and the sphere (neglecting friction actions between the sphere and the fins).
To estimate the friction contribution the tube can be assumed having a linear elastic behavior, the sphere deformation can be neglected and fundamentals equations of membrane theory of shells can be used. Stress-strain configuration in a plane orthogonal with respect to the tube axis and containing the sphere centre can be analysed.

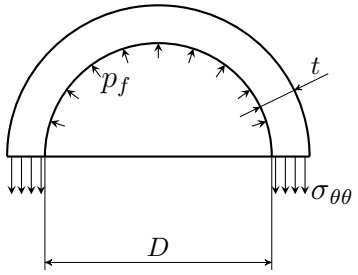

Figure 5: Stress configuration in tube section

In Fig.5, p_f represents the pressure action due to the tube deformation ($D > d_3$), $\sigma_{\theta\theta}$ represents the circumferential normal stress in the tube and t the tube thickness. The circumferential strain value $\epsilon_{\theta\theta}$ is given by the system geometry:

$$\epsilon_{\theta\theta} = \frac{2\pi D - 2\pi d_3}{2\pi d_3} = \frac{D - d_3}{d_3} \tag{8}$$

And by the constitutive equation:

$$\sigma_{\theta\theta} = E\,\epsilon_{\theta\theta} = E\,\frac{D - d_3}{d_3} \tag{9}$$

Writing the equilibrium equation with respect to a vertical direction it results:

$$2\sigma_{\theta\theta}\,t = p_f\,D \tag{10}$$

So it is possible to find the pressure value in the section plane and, by multiplying for the friction coefficient f between the sphere and the thermoplastic tube, an evaluation of the friction action:

$$\tau_f = f\,p_f = 2f\,\frac{t}{D}\,\sigma_{\theta\theta} \tag{11}$$

As mentioned above, these are the involved quantities in the specified section plane. As first approximation it is possible to extend this situation to the whole sphere-tube contact zone, that has an axial width of $x = \sqrt{D^2 - d_3^2}$. The energy dissipated by friction is:

$$W_f = \pi D x\,\tau_f\,m = 2f\pi t\,m\,E\frac{D - d_3}{d_3}\sqrt{D^2 - d_3^2} \tag{12}$$

And the energy conservation equation becomes:

$$\begin{aligned}\frac{\pi D^2}{4}(p_{\max} - p_{\text{atm}})\left(\ell + \frac{1}{2}\sqrt{D^2 - d_2^2} + m\right) = \frac{\pi E h^3 (d_1 + d_2)(D^2 - d_2^2)}{16(d_1 - d_2)^3} + \\ +2f\pi t\,m\,E\frac{D - d_3}{d_3}\sqrt{D^2 - d_3^2}\end{aligned} \tag{13}$$

The equation 13 contains several unknown parameters. It is possible to analyse their mutual dependencies.

From the energy conservation equation it is possible, for example, to find out the dependency between the initial sphere stroke and the desired penetration into the left part:

$$\ell = \frac{4}{\pi D^2 (p_{\max} - p_{\text{atm}})} \left[\frac{\pi E h^3 (d_1 + d_2)(D^2 - d_2^2)}{16(d_1 - d_2)^3} + 2f\pi\, t\, mE \frac{D - d_3}{d_3} \sqrt{D^2 - d_3^2} \right] + \\ - \frac{1}{2} \sqrt{D^2 - d_2^2} - m \tag{14}$$

Trying to estimate reasonable values for the parameters it has been possible to obtain the order of magnitude of the involved quantities and determine if this solution is physically feasible. Making use of a simple MATLAB script it is possible to plot the above expression for $\ell(m)$, for example starting from the following parameters:

- Silicone rubber with $E = 10\,\text{Mpa}$
- Sphere diameter $D = 4\,\text{mm}$
- Tube larger diameter $d_1 = 5\,\text{mm}$
- Fins inner diameter $d_2 = 3\,\text{mm}$
- Tube smaller diameter $d_3 = 3,6\,\text{mm}$
- Fins thickness $h = 1\,\text{mm}$
- Tube thickness $t = 2\,\text{mm}$
- Friction coefficient between sphere and tube $f = 0,1$

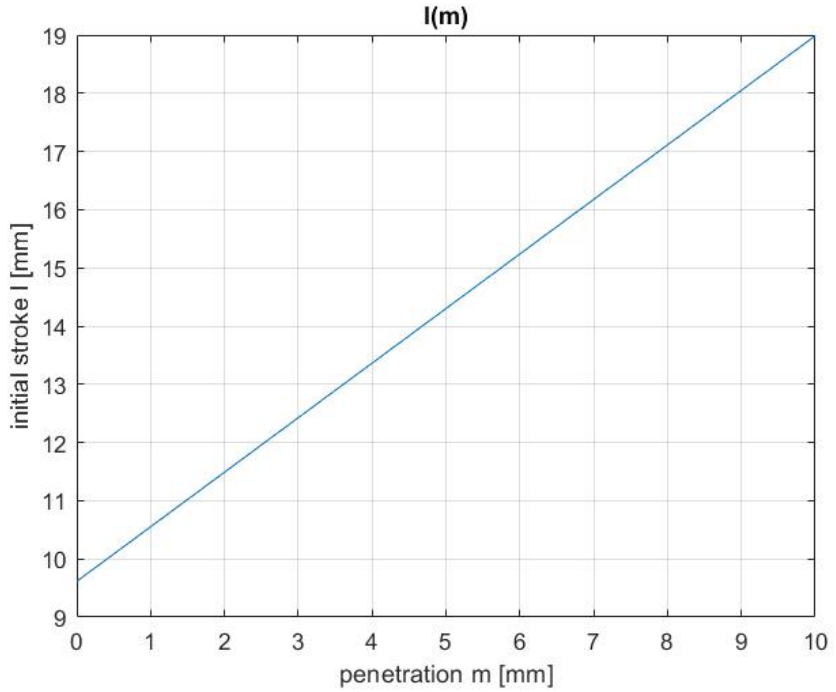

Figure 6: MATLAB plot

As it is possible to observe from the Fig.6 the solution turned out to be physically possible. In fact, although the first calculations were not completely accurate, the involved dimension

were anything but unreasonable and the results were very promising in terms of feasibility. It definitely would be interesting to deepen this analysis with more precise models and adjust them in order to obtain a practical and effective solution. However, this solution was abandoned for several reasons. Firstly it is not recommended to rely a safety mechanism on a friction related phenomenon and uncertainties about friction coefficient value make mathematical models hard to formulate without complex experimental tests. In addition, it is inconvenient to have the sphere moving during normal functioning. A track for the sphere would be necessary and there would be intrinsic difficulties to estimate the actual initial sphere stroke.

2.3 Second approach

As mentioned above, first approach basic problems were the relevant contribution of friction and the sphere continuous motion. Both caused a substantial uncertainty concerning the correct mechanism functioning.
Trying to maintain the spherical geometry and the bistable concept, a second solution has been conceived and designed. The basic idea was to consider a soft material structure able to hold the sphere in normal operating conditions and release it to obstruct the tube in case of relevant pressure gradient. A possible solution is represented in Fig.7. The soft structure holding the sphere is provided with peripheral holes with axis parallel to the tube axis to let the flow pass through during normal functioning. The sphere is not supposed to penetrate in a smaller tube but, instead, it is supposed to get in contact with the tapered part and obstruct the flow.

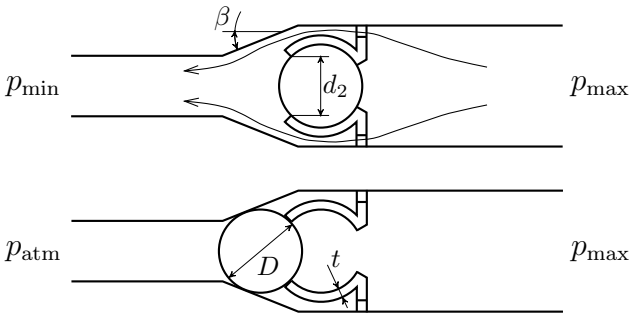

Figure 7: Second approach operating principle

For the sake of simplicity and clarity, Fig.7 is a schematic section view, so it only represents the intersection of the system with the section plane. The system is axisymmetric with respect to the tube axis (with the exception of the peripheral holes).
As in the first solution, during its way out of the elastic holding shell, the sphere deforms the structure. The geometry has to be sized in a way that the soft material holding structure, when the sphere has came out, contributes pressing it against the tapered part in order to keep the sphere in position. From geometrical considerations it is possible to relate the distance between the soft holding shell and the tapered part to the other system sizes.
With reference to the Fig.8, it is possible to relate the size m to the other geometrical quantities, in particular to the covering angle γ of the soft holding shell (so to the diameter d_2) and to the opening angle β of the tapered part. This is not a convenient technological dimension because of its verification difficulty, but provides an idea of the axial positioning of the various system parts. Obviously the covering angle γ is related to the sphere diameter and the shell opening diameter: $\cos\gamma = \frac{d_2}{D}$. It can be written:

$$m \leq \frac{1}{2}(D\cos\beta - d_3)\frac{1}{\tan\beta} + \frac{D}{2}\sin\beta + \frac{D}{2}\sin\gamma \tag{15}$$

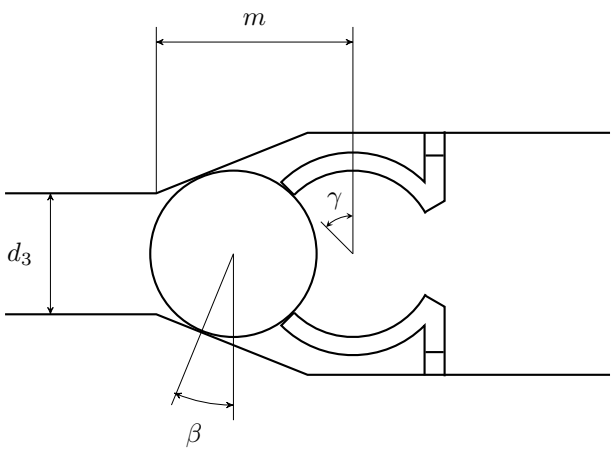

Figure 8: Scaled representation of the system

Or equivalently:

$$m \leq \frac{1}{2}(D\cos\beta - d_3)\frac{1}{\tan\beta} + \frac{D}{2}\sin\beta + \frac{1}{2}\sqrt{D^2 - d_2^2} \tag{16}$$

Where the inequality is necessary if the soft shell is desired to keep the sphere in position.
With the aim of writing a simple relation between the involved quantities, as for the first approach, energy conservation can be written. Taking into account a consistent error, membrane theory of elastic shells can be used and friction can be neglected.
When the damage occurs, during its axial motion the sphere deforms the soft material shell. Considering the greater deformation situation, the shell opening is stretched out in order to let the sphere pass through. Quantitatively, the opening diameter increases from d_2 to D. Assuming the shell deformed region to have an axial extension of $\frac{D}{2}\sin\gamma = \frac{1}{2}\sqrt{D^2 - d_2^2}$ (axial sphere displacement when greater deformation occurs), the circumferential strain is:

$$\epsilon_{\theta\theta} = \frac{D - d_2}{d_2} \tag{17}$$

So the circumferential normal stress:

$$\sigma_{\theta\theta} = E\,\epsilon_{\theta\theta} \tag{18}$$

And the elastic energy in the shell deformed region:

$$W_{el} = \frac{1}{2}\sigma_{\theta\theta}\,\epsilon_{\theta\theta}\,\pi D\,t\frac{1}{2}\sqrt{D^2 - d_2^2} = \frac{\pi}{4}ED\,t\frac{(D - d_2)^2}{d_2^2}\sqrt{D^2 - d_2^2} \tag{19}$$

And for the energy conservation principle this is equal to the pressure work:

$$\frac{\pi D^2}{4}(p_{\max} - p_{\text{atm}})\frac{1}{2}\sqrt{D^2 - d_2^2} = \frac{\pi}{4}ED\,t\frac{(D - d_2)^2}{d_2^2}\sqrt{D^2 - d_2^2} \tag{20}$$

And by simplifying:

$$\frac{D}{2}(p_{\max} - p_{\text{atm}}) = Et\,\frac{(D - d_2)^2}{d_2^2} \tag{21}$$

As for the first approach, a relation between two unknown quantities can be made explicit, plotted and analysed with the other parameters varying in order to determine with very coarse approximation the feasibility of the solution.

For example, the shell opening diameter d_2 can be made explicit varying the sphere diameter D and the other parameters can be reasonably estimated. Making use of a MATLAB script for $d_2(D)$ and assuming the following parameters values:

- Silicone rubber with $E = 0,1\,\text{Mpa}$
- Holding shell thickness $t = 0,5\,\text{mm}$

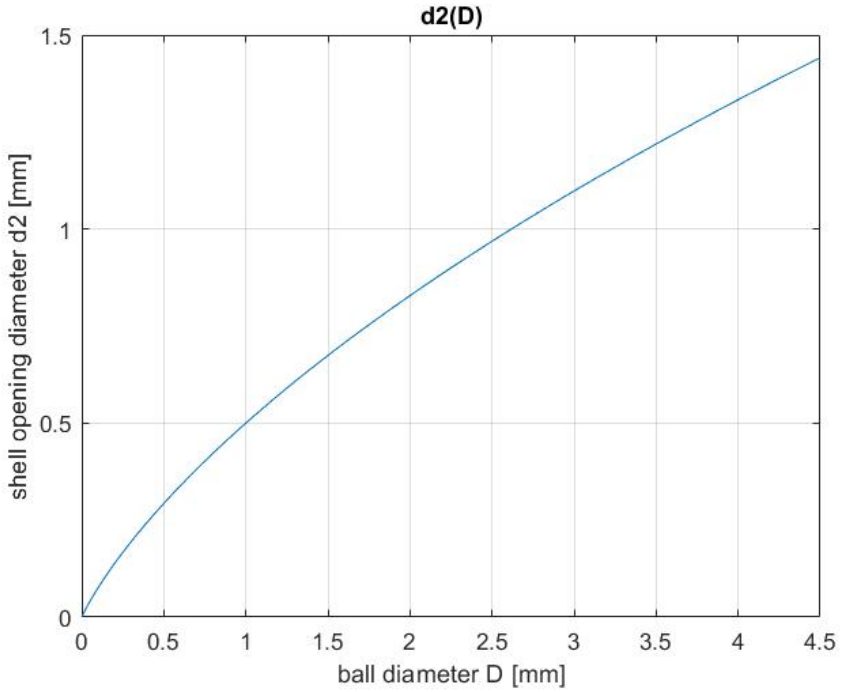

Figure 9: MATLAB plot

Observing the diagram in Fig.9, also this second approach seemed very promising in terms of feasibility. This solution provides less uncertainties compared to the firs one, because the sphere is held fixed, the friction is less relevant and the shell contributes keeping the sphere in position when obstructing the downstream tube.

2.4 Fluidic model

In order to make an evaluation of the hydraulic behavior of the system, approximated fluidic calculations can be developed. In the previous section the assumption that the force acting on the sphere can be expressed as $F_p = \frac{\pi D^2}{4}(p_{\max} - p_{\text{atm}})$ has been done. This assumption can be verified taking into account the fluid viscosity properties and estimating the force of interaction between the flow and the sphere.
The flow values involved during system normal functioning and in the catastrophic rupture situation depend on the geometrical characteristics of the circuit and on the operating pressures. The system that has to be analysed is a single branch, schematized in Fig.10. It consists, as previously described, of tubes of diameter $d = 2\,\text{mm}$, the valve (double triangle symbol) and the McKibben actuator (which is represented as a variable volume $V(t)$).
The valve can be associated to its equivalent length ℓ_{eq}, defined as the length of straight tube that produces the same pressure loss in the circuit. The use of this parameter entails an approximations in calculations an the result will be accurate only concerning the order of magnitude. In fact, a precise value for ℓ_{eq} can be obtained only from experimental measures

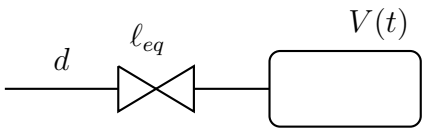

Figure 10: Branch scheme

and is unnecessary for this model. A coarse value for ℓ_{eq} can be found in the catalogues of valve manufacturers, who provide nomograms that return it based on the tube diameter and the valve type. In the specific case the valve can be compared to a standard sphere check valve and a reasonable value turns out to be $\ell_{eq} = 0,1\,\mathrm{m}$.
The variable volume $V(t)$ is the element that requires the oscillating pressure and the flow rate in the circuit. For the approximated model it can be visualized as a sinusoidal function between the two values of $V_{min} = 0,8\,cm^3$ and $V_{max} = 2.4\,cm^3$, that is plotted in Fig.11.

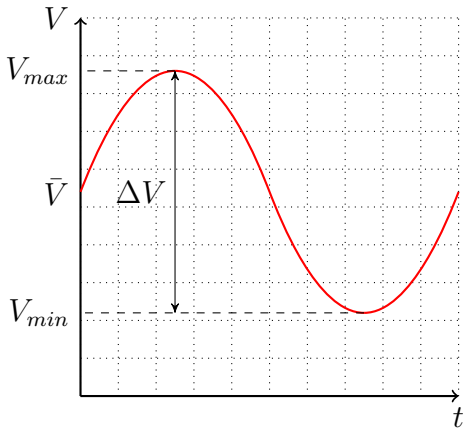

Figure 11: Evolution over time of a McKibben muscle volume

$$V = \bar{V} + \frac{\Delta V}{2} \sin\left(\frac{2\pi}{T} t\right) \tag{22}$$

The frequency of the sine curve is $f \simeq 1\,\mathrm{Hz}$, so the period $T \simeq 1\,\mathrm{s}$. Deriving $V(t)$ with respect to the time it is possible to express the maximum value of the flow rate:

$$Q_{max} = \pi \frac{\Delta V}{T} \simeq 5\,\mathrm{cm}^3 \cdot \mathrm{s}^{-1} \tag{23}$$

And the maximum fluid velocity turns out to be:

$$w_{max} = \frac{4Q_{max}}{\pi d^2} \simeq 1,6\,\mathrm{m} \cdot \mathrm{s}^{-1} \tag{24}$$

Assuming the fluid to be water, in the range of temperature $T = 20 \div 40°\mathrm{C}$, it is possible to consider a density $\rho = 10^3\,\mathrm{kg} \cdot \mathrm{m}^{-3}$ and a dynamic viscosity of $\nu = 10^{-3}\,\mathrm{Pa} \cdot \mathrm{s}$.
Calculating the Reynolds Number:

$$Re = \frac{\rho w_{max} d}{\nu} = 3200 \tag{25}$$

So the flow, in a system composed by only a straight tube of length ℓ_{eq}, would be described by a laminar-turbulent transition. With a turbulent flow, the pressure drop in a tube depends on the tube's internal surface roughness by a "friction coefficient" f that is possible to obtain

from the well known Moody diagram. For the sake of simplicity and approximation, taking into account that the tubes are made of thermoplastic material, it is possible to neglect the internal roughness, obtaining, for $Re = 3200$, $f = 0,04$. The pressure drop on the valve in this situation turns out to be:

$$\Delta p = f\frac{\ell_{eq}}{d}\rho\frac{w_{max}^2}{2} \simeq 0,025\,\text{bar} \tag{26}$$

And from this result, knowing the flow rate and the pressure loss, it is possible to evaluate the characteristic constant of the valve:

$$K_v = \frac{Q_{max}}{\sqrt{\Delta p}} = 3,2 \cdot 10^{-5}\,\text{m}^2 \tag{27}$$

It is possible now to consider the catastrophic rupture of the actuator ($\Delta p' = 1\,\text{bar}$):

$$Q' = K_v\sqrt{\Delta p'} \simeq 32\text{cm}^3 \cdot \text{s}^{-1} \tag{28}$$

$$w' = \frac{4Q_{max}}{4d^2} \simeq 10,1\,\text{m} \cdot \text{s}^{-1} \tag{29}$$

$$Re' = \frac{\rho w' d}{\nu} = 28000 \tag{30}$$

So, as showed by the Reynolds Number, in this situation the flow is turbulent. To have a coarse evaluation of the force acting on the sphere, it is possible to apply the formula for the force exerted by an infinite fluid on a sphere in turbulent motion:

$$F_v = \frac{\pi}{8}C_r\rho D^2 w'^2 \simeq 0,1\,\text{N} \tag{31}$$

Where $D = 2,5\,\text{mm}$ is the sphere diameter and $C_r = 0,4$ is a shape coefficient for the spherical geometry. It is possible to notice that the order of magnitude of the result is the same of the calculation of the force from the pressure gradient:

$$F_p = \frac{\pi D^2}{4}\Delta p' \simeq 0,5\,\text{N} \tag{32}$$

So the model is consistent. It is important to observe that from the previous calculations an indirect "proof of safety" has been obtained. In fact, during normal functioning, the pressure drop on the valve is around one hundred times smaller than the one that should push the sphere out of the hyperelastic structure. Therefore, it is impossible for a branch to be obstructed without the McKibben muscle damage.
In the next section a deeper analysis and design of this structure has been developed. SolidWorks and ANSYS Workbench have been used for this purpose.

3 Mechanical design

The system has been designed with the aim of simple technological realization and an easy integration in an existing pneumatic circuit. The idea was to develop an assembly composed by several elements to be inserted and blocked in the circuit tubes. The starting data are the tubes characteristics, which consist of thermoplastic material, inner diameter of 2 mm and outer diameter of 4 mm. Some pictures of the final CAD models are displayed below.

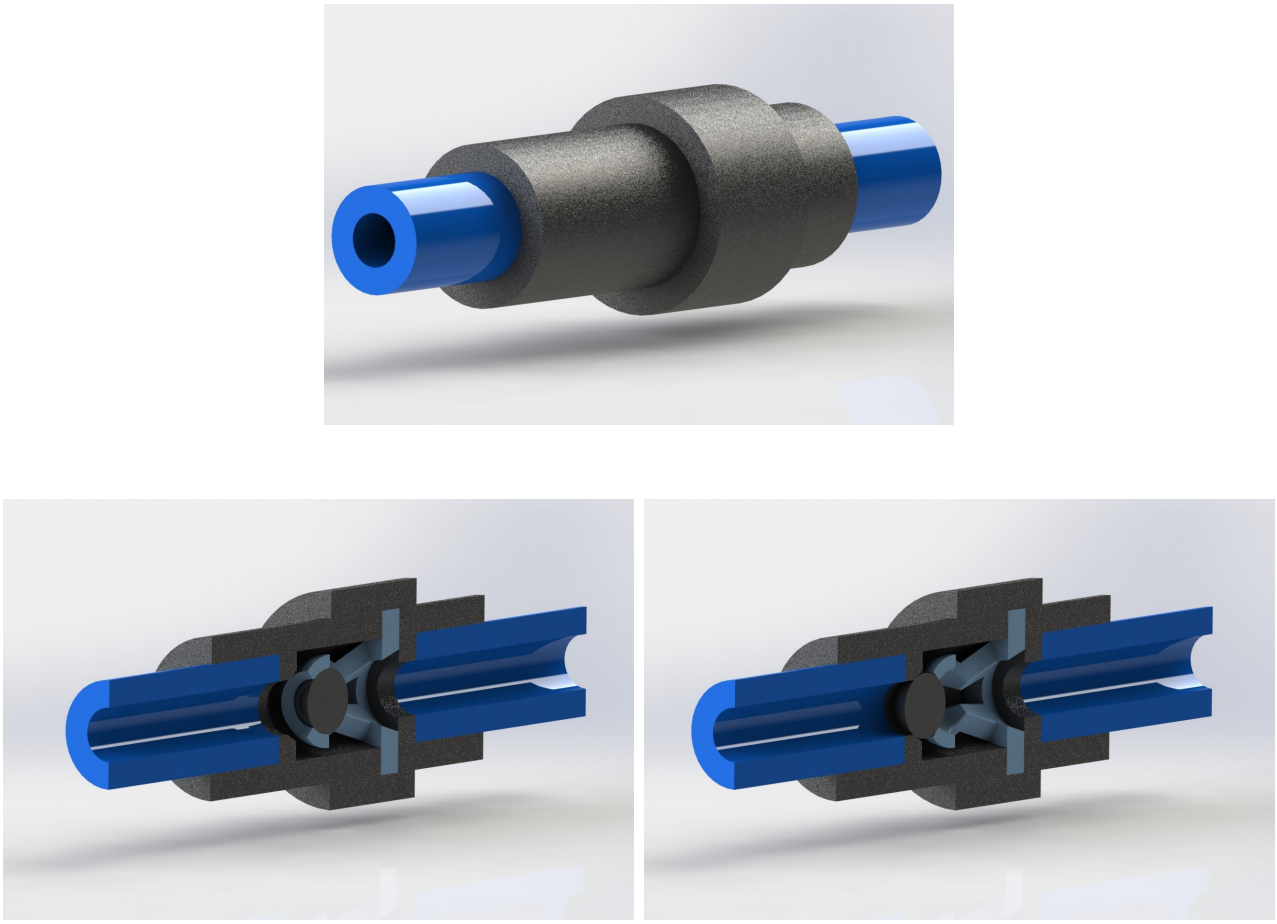

Figure 12: Final Assembly

In Fig.12 the whole system is represented and the connection with the tubes can be observed. Unfortunately the tubes are too small to entirely contain the valve assembly, so the structure has a greater radial overall dimension with respect to the tubes. The two outer black elements are made of stiff thermoplastic material (Delrin) and are necessary for the fastening with the tubes. Moreover, they hold in position the soft material element (light blue). The section pictures represent the two possible sphere positions. The normal functioning position on the left and the obstructing position on the right.

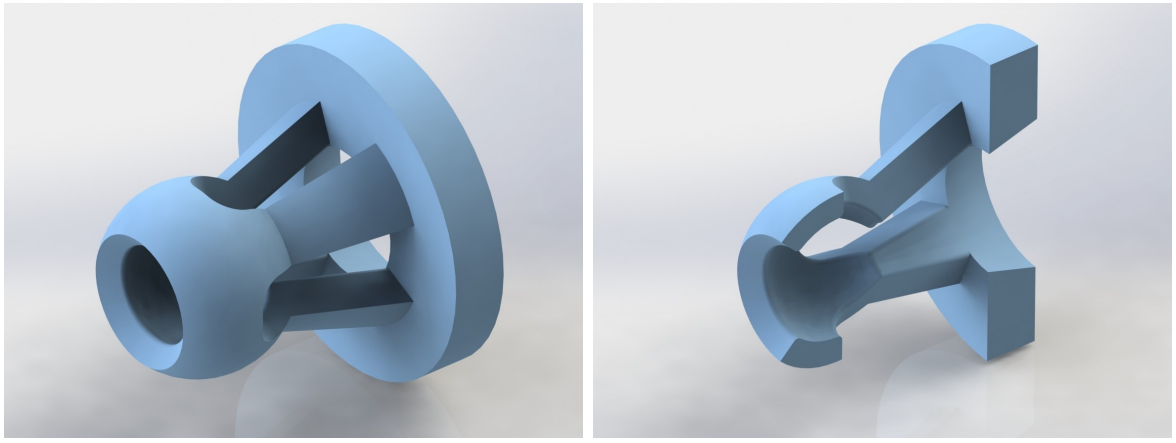

Figure 13: Soft material valve

The soft material element, as illustrated in Fig.13, has been modified in order to be easily disassembled if necessary. The spherical cavity correspond to the holding shell. The inlet part is tapered in order to interfere as little as possible with the flow. The lateral holes have been replaced with peripheral slots. The mechanical and structural characteristics of this component have been determined with load simulations in ANSYS Workbench.

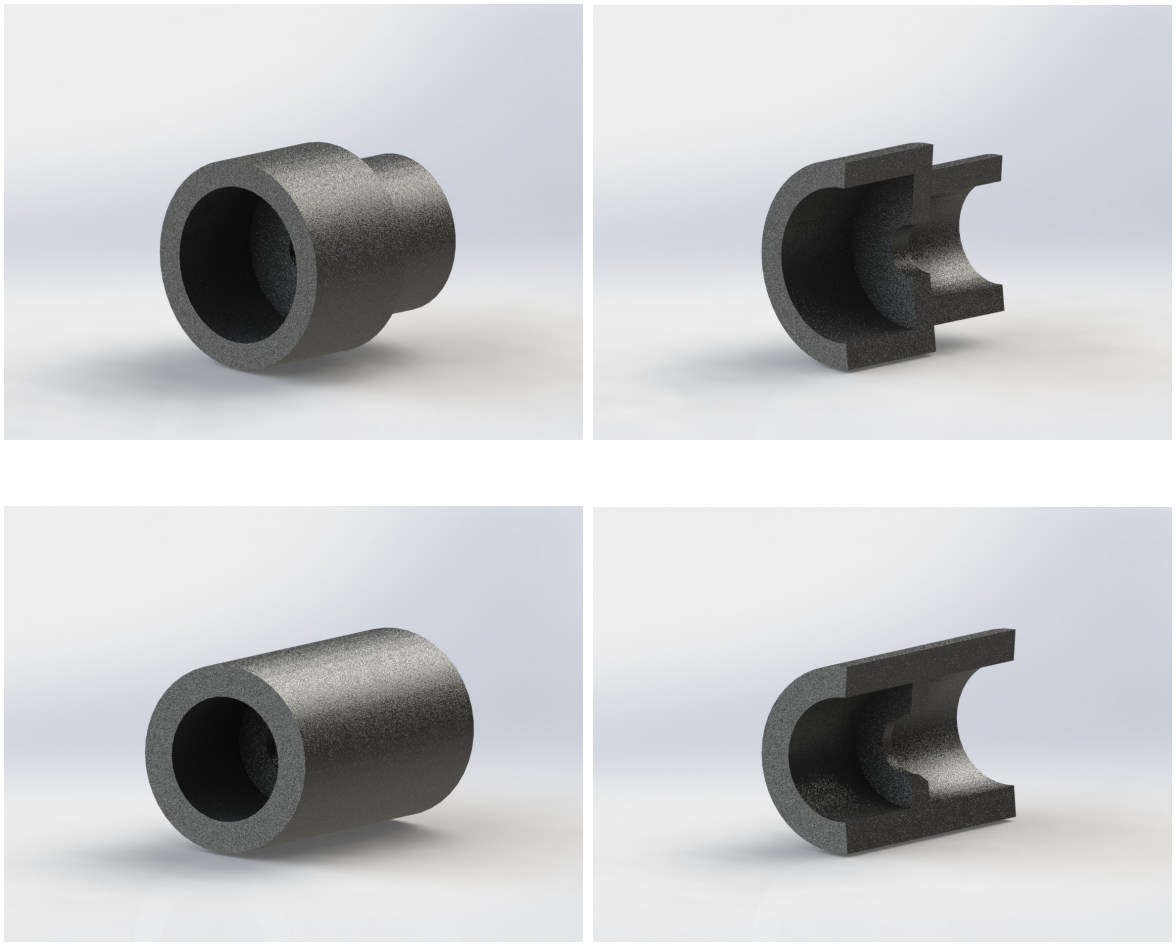

Figure 14: Stiff Delrin elements

The two stiff elements (Fig.14) are realized by lathing. The axial dimensions are calculated in order to guarantee the pressing action of the soft valve on the sphere in the obstructing position. The second stiff element (lower pictures) is provided with a chamfer with the goal of ensuring a correct contact with the sphere in the obstructing position.

4 FEM simulations

In this section the results of the Finite Element Analysis are reported. The basic assumptions are explained and the consistency with the approximated calculations is verified.

4.1 Load simulation

On ANSYS Workbench a "trial and error" analysis has been conducted, trying to simulate the behavior of a soft valve given geometry and making corrections based on the simulation results. The geometry was imported from the SolidWorks assembly and all the components were suppressed except for the soft material element and the sphere. The simulation type was chosen as transient structural.
Indeed, the facing problem involves large displacements and deformations, and several time steps are suitable. The lateral surface of the valve base has been set up as fixed support (in fact when assembled on the tubes it is blocked by the two stiff components). The contact between the sphere and the holding shell was set as frictional, with a friction coefficient of 0.1. An axial displacement was imposed to the sphere (10 time steps, 0.15 mm displacement each) and a probe measuring the force reaction on the fixed support was inserted. In Fig.15 the soft element mesh is showed.

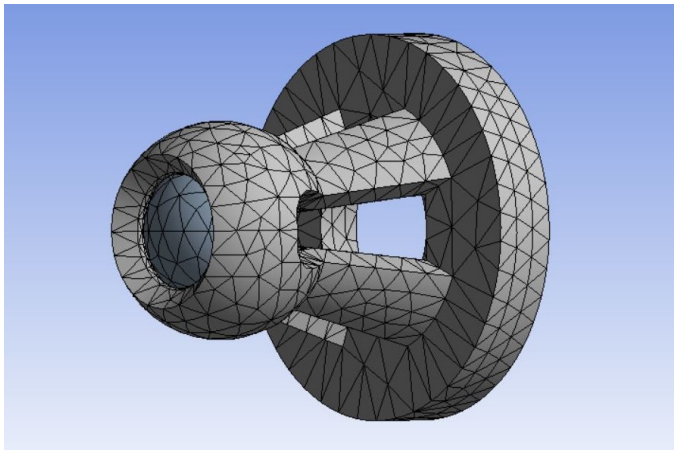

Figure 15: Simulation mesh

Comparing the measured force with the expected action caused by the pressure gradient several geometry modifications were made. In particular, a shell thickness greater than 0.5 mm didn't affect considerably the force opposed to the sphere motion. The lower bound was imposed by technological issues. In fact the valve shape has to be obtained by silicone injection in a mold and there are limitations on the achievable thicknesses. The other parameter corrected were the Young modulus of the soft material (from which the silicone type was chosen) and the shell opening diameter. In particular, it was noticed that with a friction coefficient of 0.1 the maximum covering angle γ allowing the sphere exit was around 55°.
The following Fig.16 shows the graphical output of a simulation with parameters defined as:

- Shell thickness $t = 0.5\,\text{mm}$
- Friction coefficient $f = 0.1$
- Covering angle $\gamma = 45°$
- Material Young modulus $E = 1\,\text{Mpa}$
- Sphere diameter $D = 2.5\,\text{mm}$

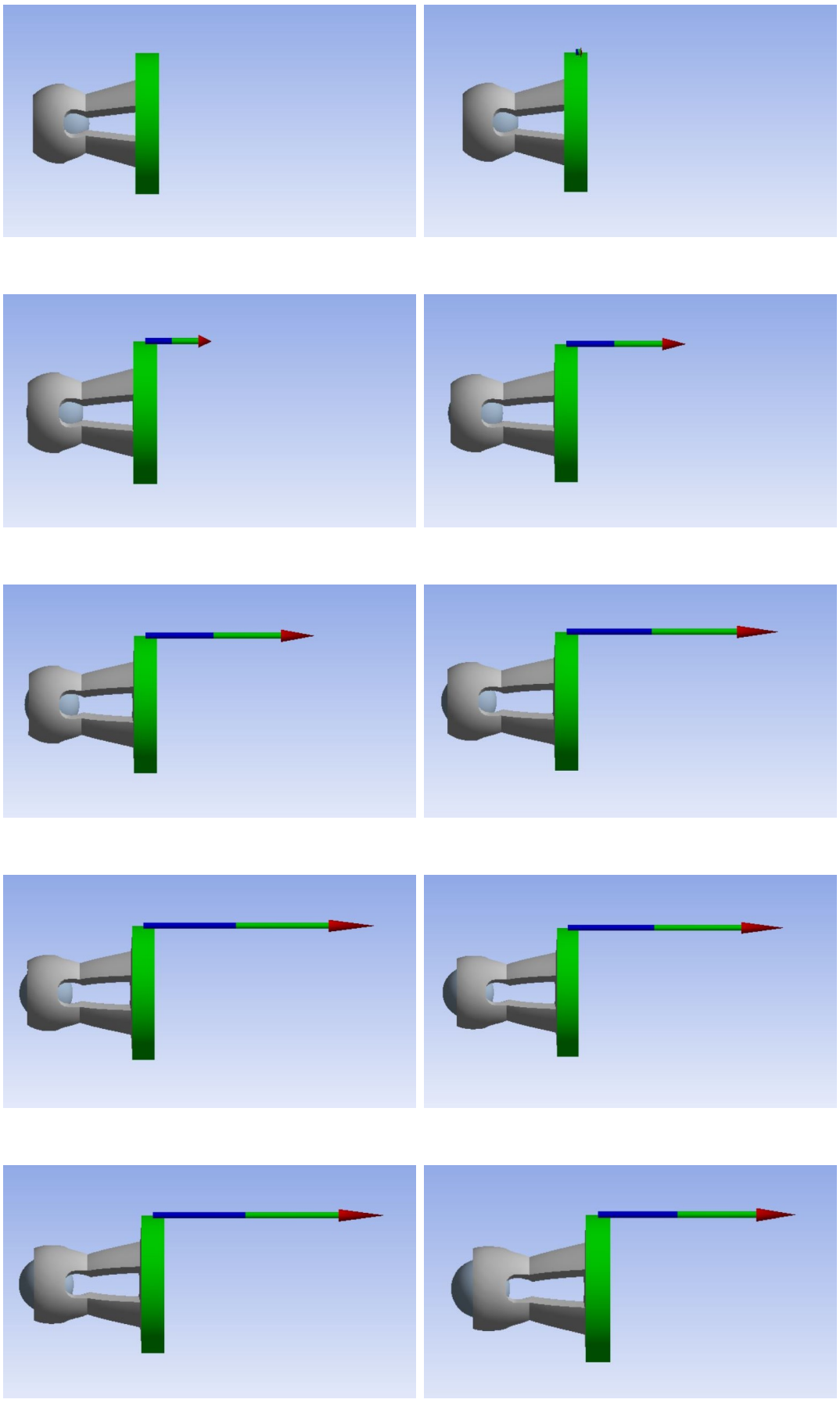

Figure 16: Load simulation graphic output

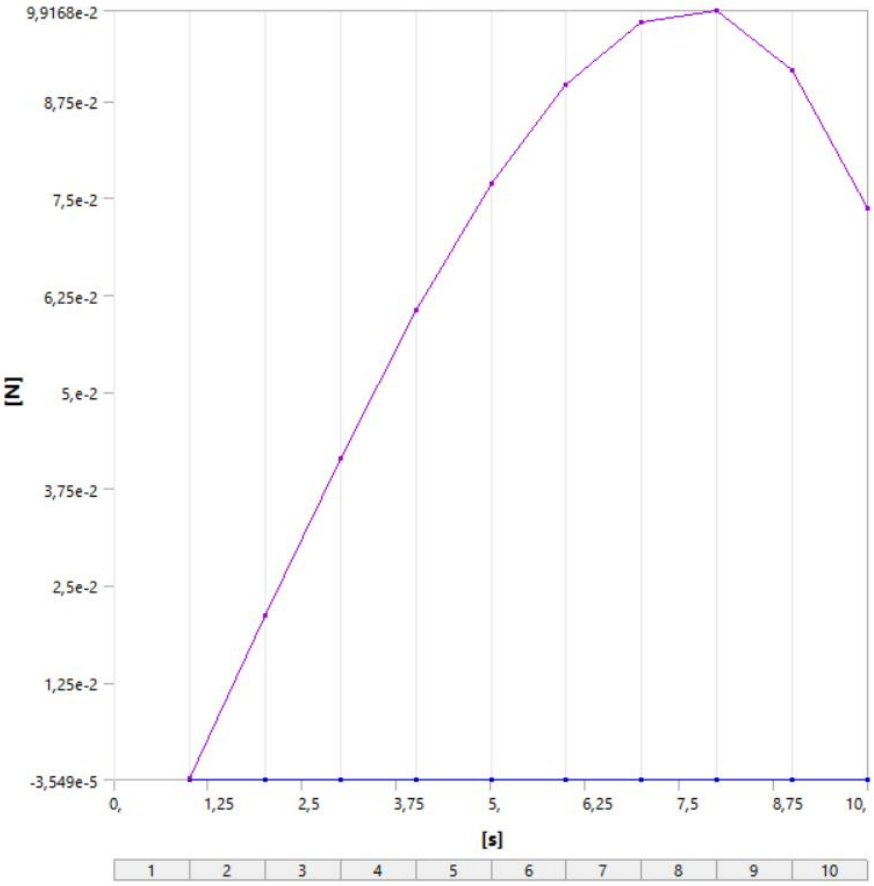

Figure 17: Axial force reaction values

As it can be observed by the simulation diagram in Fig.17, the maximum reaction force has the same order of magnitude of the previously computed F_p and F_v:

$$F_{max} \simeq F_p \simeq F_v \tag{33}$$

Thanks to simulation results the material and the shell thickness have been decided. In particular the chosen silicone is the Smooth-Sil 950[1] (100% strain Young modulus $E_{100\%} = 1.88\,\text{Mpa}$) and the final shell thickness $t = 0.5\,\text{mm}$.

Density	Pot Life	Cure Time	Shore A Hardness	Tensile Strength	100% Modulus	Elongation at Break
$1.24\,\text{g cm}^{-3}$	45 min.	18 hrs.	50 A	5.0 Mpa	1.87 Mpa	320%

Silicone rubbers are hyperelastic materials, so, assuming a constant Young modulus for calculations and simulations, a modelling approximation error has to be taken into account. For hyperelastic materials the Young modulus is a function depending on the strain condition $E(\epsilon)$. In this particular case, the maximum equivalent strain of the shell is approximately:

$$\epsilon_{\text{eq}} \simeq \epsilon_{\theta\theta} = \frac{D - d_2}{d_2} = 1 - \frac{1}{\sqrt{2}} \simeq 0.3 \tag{34}$$

so the linear elastic model is acceptable.
Unfortunately the friction between the sphere and the shell causes a consistent uncertainty about the system behavior. It depends on the sphere material, that is steel (easy to buy from bearing producers), but remains an unknown parameter. For this reason experimental trials on

[1] `https://www.smooth-on.com/products/smooth-sil-950/`

the system are necessary and the last parameter that needs to be determined is the holding shell covering angle γ. In the next section the mold for silicone injection design will be illustrated, paying attention to a modular component that allows to obtain from the same mold valves with different covering angle values.

4.2 Fluidic simulation

On ANSYS Fluent a single simulation has been developed. The only objective was to verify the level of approximation of the basic hydraulic calculations. The CAD model of the fluid volume in the system has been created and imported to Harpoon for the mesh generation. As represented in Fig.18 the employed mesh is a hexahedral type mesh.

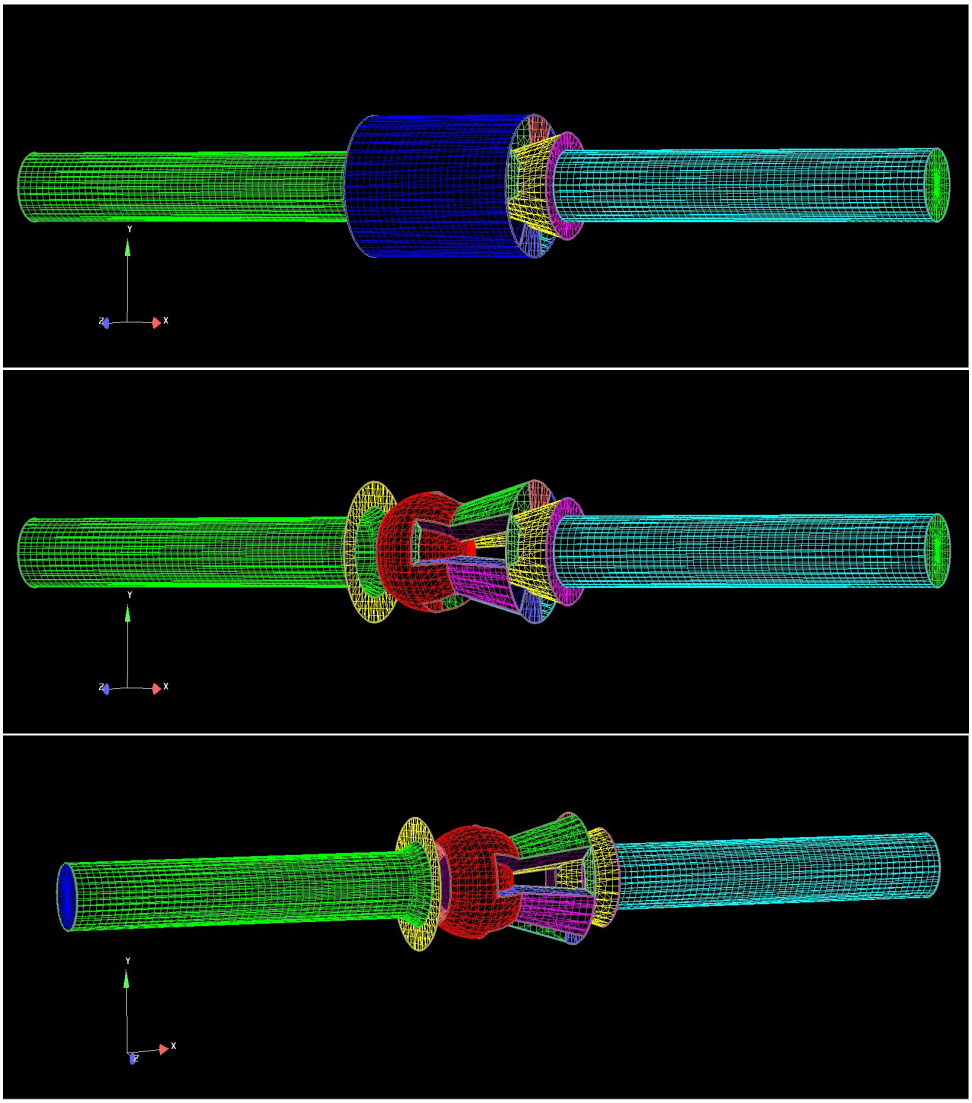

Figure 18: Mesh for the fluidic computation

Inlet an outlet sections consist of the tubes extremities. The system analysis does not require any particular precaution concerning the model, so no specific parameters have been changed in the solution setup. The solution was calculated for steady flow conditions making use only of the viscous model of liquid water in standard conditions. For the turbulence, the $k-\epsilon$ model has been utilized. The boundary conditions have been imposed to inlet and outlet sections with the pressure difference of 1bar.
The results of the simulations have been astonishing compliant with the approximated hydraulic model (section 2.4). In Fig.19 it is possible to observe the static pressure and the velocity

contours of the water in the tubes and around the valve elements (pressures are relative values and referred to the atmospheric pressure).

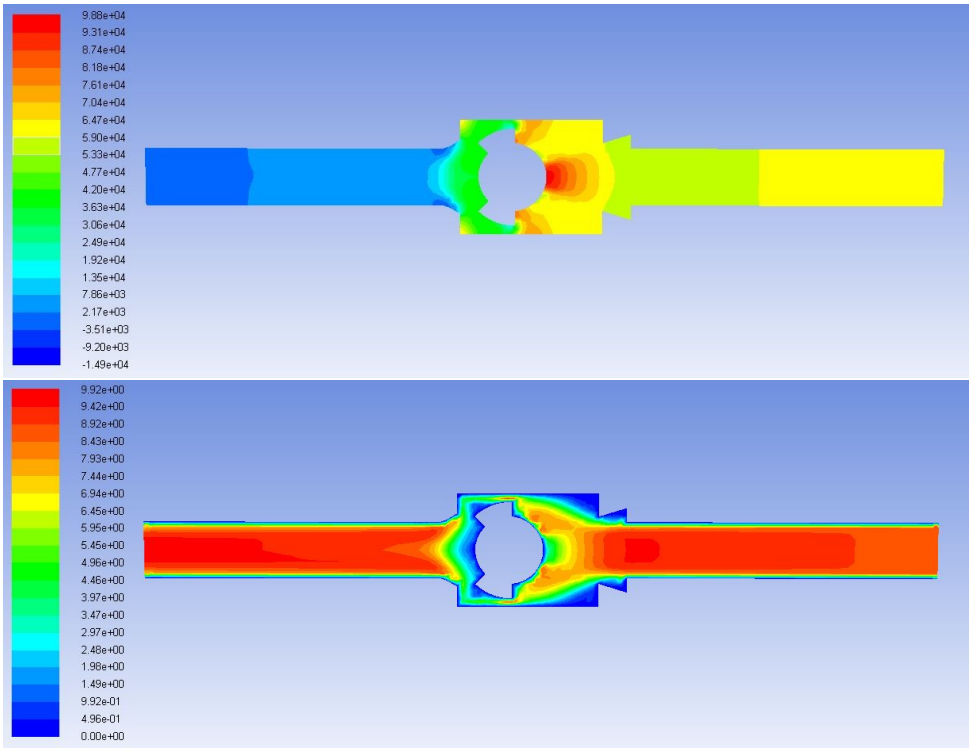

Figure 19: Static pressure and velocity contours

Moreover, in post processing it is possible to compute the forces produced by the fluid on the mesh elements. In particular, it has been possible to calculate the force on the sphere adding up the various contributions on the mesh surfaces that compose the sphere. In this case the sphere is composed by two different surfaces (in the mesh file, 29 is the downstream half and 30 the upstream one). The result of the force report is displayed in Fig.20.

```
Forces - Direction Vector (1 0 0)
                          Forces (n)
Zone                      Pressure        Viscous         Total
solid_blocco_sim:29       0.084658116     8.1699163e-06   0.084666286
solid_blocco_sim:30       -0.19299939     -0.00057813956  -0.19357753
------------------------- --------------- --------------- ---------------
Net                       -0.10834128     -0.00056996964  -0.10891125
```

Figure 20: Calculation of the axial force on the sphere

As it is possible to observe, the solver adds up the viscous and the pressure force components. The contributions on the two sphere parts are opposite and the resultant force is of $\simeq 0,1\,\mathrm{N}$ (the flow direction is opposite with respect to the x axis).

5 Mold design

As already clarified, the silicone valve had to be obtained by mold injection. The mold was realized by 3D printing and had to be designed in order to satisfy some practical requirements. The extraction of the component had to be possible (all the undercuts have to be resolved) and easy without uselessly complicating the mold geometry. Silicone is poured in liquid state and after the polymerization reaction has taken place the extraction process is complicated and very delicate. For this reason it is suitable to have the mold divided in several parts.
In this particular case, the pouring position have been decided in order to have the element axis in vertical direction, and the greater radius part on the top. In this way it is easier to eliminate potential disturbing air bubbles from the poured liquid. The valve is provided with four lateral slots, so four lateral elements are necessary for the mold. The soft valve has small dimensions, but the mold components have to be sized for an easy handling. The quantity of employed 3D printing material is not binding. The components have to be reciprocally locked with bolts, so mold elements have to be provided with reference and blocking surfaces and ledges.

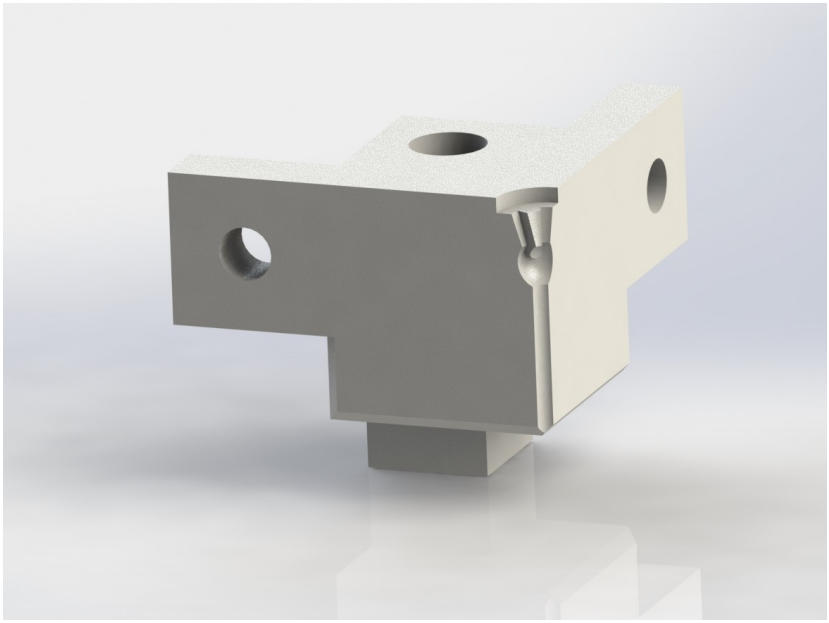

Figure 21: Lateral mold component

Fig.21 represents one of the four lateral mold components (all four are identical). It is possible to observe the quarter of the valve shape, the two holes for the bolt locking with the two adjacent components and the lower support to place the mold on a horizontal surface. Moreover, it has to be noticed the groove (45° chamfer) obtained on the lower edges of the element. These grooves are useful to leverage them with a sharp object. The valve tapered internal part can be obtained with a cone, that can be incorporated in a lid (Fig.22). References between the lid and the lateral components are four cylindrical sticks, that fit in the lateral component top surface hole. This fitting allows also to set up the tapered element penetration. The lid has to be added to the mold assembly after the liquid has been poured. The four reference cylindrical sticks provide a certain distance between the lid and the lateral mold components in order to facilitate the mold opening. Mating between the cylindrical sticks and the respective holes has to be precise for a correct reference between elements.
The last mold component is the one that allows obtaining valves with different covering angle γ from the same mold. It is composed by a lower cylindrical part, that mates with the cylindrical shape under the valve quarter shape in the lateral mold components, and a two diameters spherical part. The greater diameter part mates with the spherical surface of the

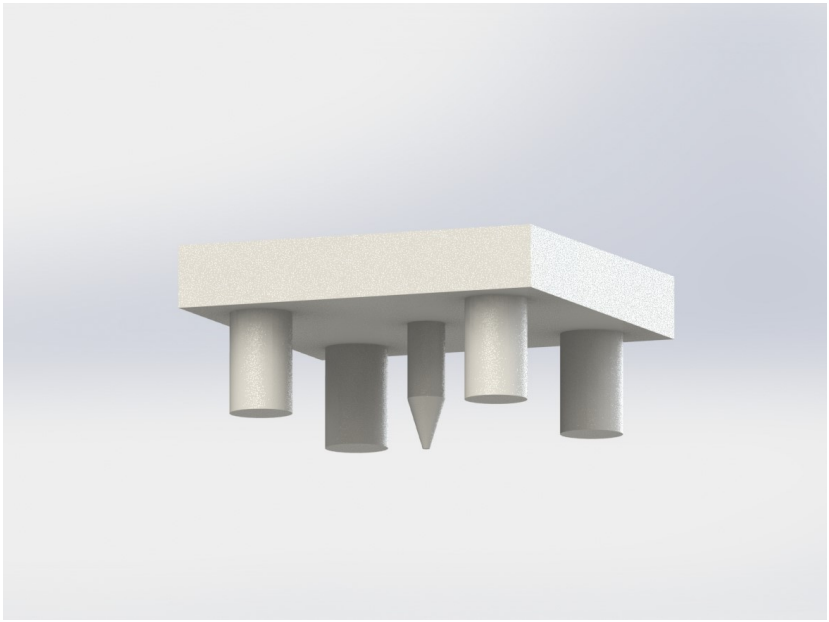

Figure 22: Lid with tapered element

lateral components that generates the external surface of the valve holding shell. As showed in Fig.23, the smaller diameter part generates the sphere compartment in the valve. The modular element is provided with a tapered hole for mating with the lid's tapered element.

Figure 23: Modular element

It is sufficient to produce several modular elements with different covering angle γ and insert them in the mold to obtain different valve shapes. The concept is showed in Fig.24.

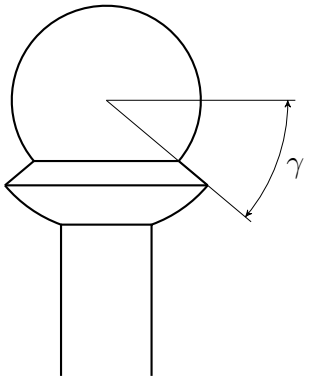

Figure 24: Covering angle on the modular element

The mold assembly is represented in Fig. 25. As it can be observed the sizes are considerably greater with respect to the valve ones.

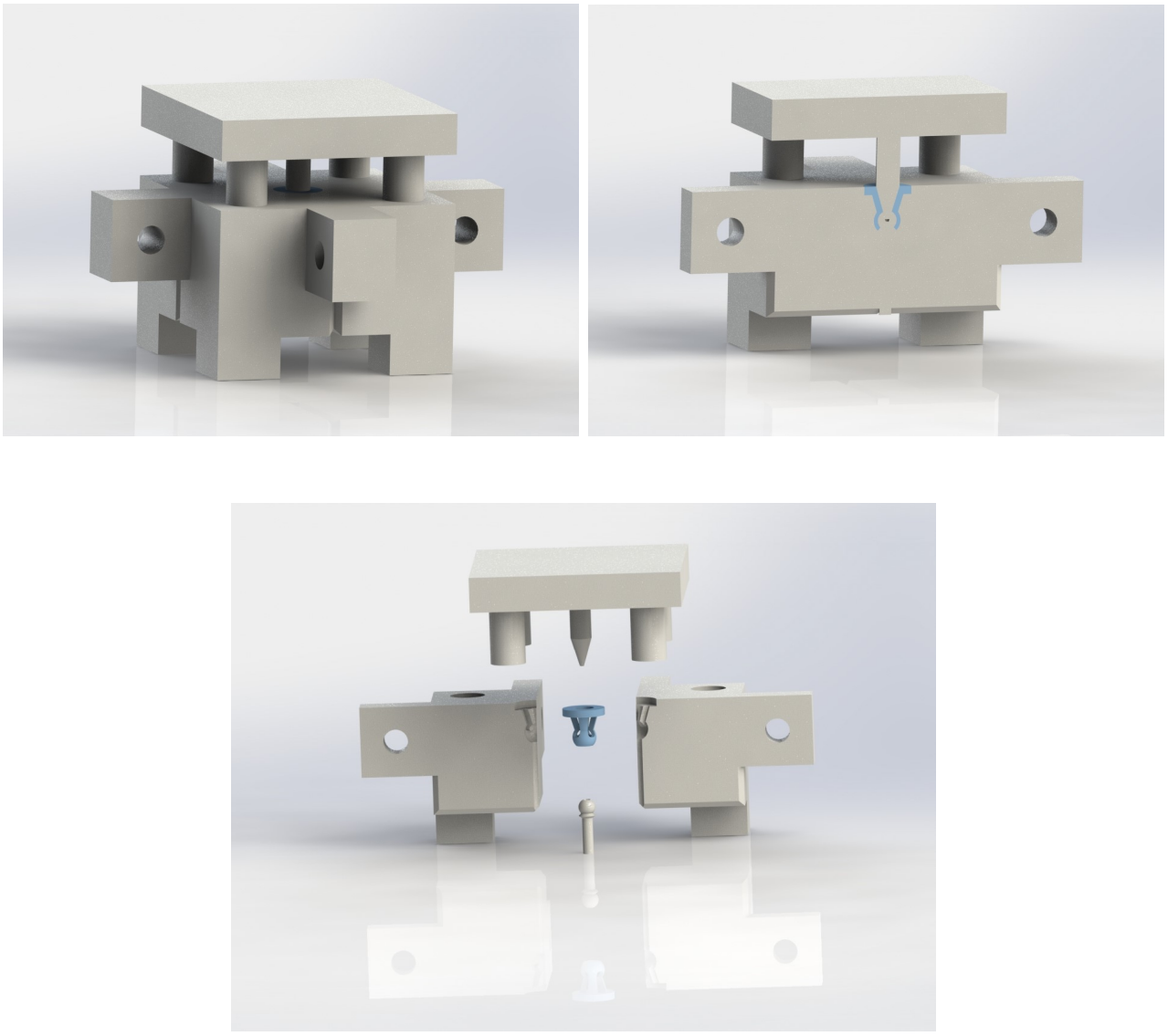

Figure 25: Mold assembly

After the production of the several valves with different sphere covering angle it is necessary to proceed with the experimental tests in order to understand which values of γ guarantee a correct functioning with the specific (unknown) friction coefficient between sphere and valve.

References

[1] N. Napp, B. Araki, M. T. Tolley, R. Nagpal, and R. J. Wood. "Simple Passive Valves for Addressable Pneumatic Actuation". In: *IEEE International Conference on Robotics & Automation* (2014), pp. 1440–1445.

[2] M. D. Gilbertson, G. McDonald, G. Korinek, J.D. Van de Ven, and T. M. Kowalewski. "Soft Passive Valves for Serial Actuation in a Soft Hydraulic Robotic Catheter". In: *Journal of Medical Devices* 10.030931 (2016).

[3] R. F. Shepherd, A. A. Stokes, J. Freake, J. Barber, P. W. Snyder, A. D. Mazzeo, L. Cademartiri, S. A. Morin, and G. M. Whitesides. "Using Explosions to Power a Soft Robot". In: *Angewandte Chemie International Edition* 52.10 (2013), pp. 2892–2896.

[4] X. Jiang and P. B. Lillehoj. "Pneumatic Microvalves Fabricated by Multi-material 3D Printing". In: *IEEE 12th International Conference on Nano/Micro Engineered and Molecular Systems* (2017), pp. 38–41.